Single-Source Vacuum Deposition of Mechanosynthesized Inorganic Halide Perovskites

Yousra El Ajjouri,[†] Francisco Palazon,[†*] Michele Sessolo,[†] and Henk J. Bolink[†]

[†] Instituto de Ciencia Molecular, ICMol, Universidad de Valencia, C/ Catedrático J. Beltrán 2, 46980 Paterna, Spain

Abstract: Fully inorganic cesium lead halide perovskite thin films were prepared by an easy, fast and dry process based on single-source vacuum deposition. We investigated the structural and optical characteristics of the so-formed films as a function of chemical composition (chloride, bromide and iodide films were formed), post-deposition thermal annealing, as well as previous mechanosynthesis of perovskite powders. We found out that the $CsPbX_3$ perovskite was preferentially formed for the smaller halides and favored by previous ball-milling of CsX and PbX_2 precursors. When bigger halides were used and/or CsX and PbX_2 precursors were simply mixed without previous mechanosynthesis, PbX_2-rich compounds such as $CsPb_2X_5$ were preferentially formed in the thin films.

In the field of perovskite optoelectronics, organic-inorganic hybrid perovskites (OHPs) have been widely studied due to their attractive optical and electronic properties.[1,2] However, drawbacks such as their environmental instability due to the high volatility and moisture sensitivity of the organic compounds, might hinder the development of stable OHP optoelectronic devices.[3,4] For this reason, the more thermally stable cesium-based all-inorganic halide perovskites are being investigated.[5–9] However, conventional solution-processing for Cs-based perovskite synthesis is rather challenging due to the poor solubility of cesium halides in common solvents.[10,11] Vacuum deposition is an alternative method which allows the formation of high-quality perovskite thin films in dry process without the need of extra chemicals (*e.g.*, solvents) other than the salt precursors that form the perovskite compounds.[12] For standard dual-source thermal vacuum deposition of an ABX_3 perovskite (where A is a monovalent cation, B is a divalent metal and X the halide), AX and BX_2 precursors are simultaneously co-evaporated from two different sources.[13,14] In this case, the evaporation rates of both precursors need to be well adjusted in order to obtain the desired final composition in the film. Single-source vacuum deposition (SSVD) represents an interesting alternative to dual-source deposition due to its simplicity and speed.[15,16] Hereafter we have fabricated thin films of different cesium lead halide compounds by SSVD of CsX and PbX_2 (X = Cl, Br, and I) precursors simply mixed in a crucible. Furthermore, we have conducted dry mechanosynthesis of $CsPbX_3$ perovskites by ball-milling. This technique has recently been used for the synthesis of different hybrid and inorganic halide perovskites both in the form of colloidal nanocrystals and bulk powders.[17–20] Again, thin films were made by SSVD of these pre-synthesized perovskite powders. By performing a detailed and systematic structural and optical analysis we analyzed the different thin films that are formed through SSVD of pristine as well as ball-milled chloride, bromide, and iodide precursors at room temperature as well as upon thermal annealing.

First, thin films were prepared by SSVD of simply mixed CsX and PbX_2 precursors. Figures 1 and 2 show the structural and optical characterization of the films as-prepared at room temperature as well as after thermal annealing at 225 °C for X = Cl and Br (for X = I see Figure S2).

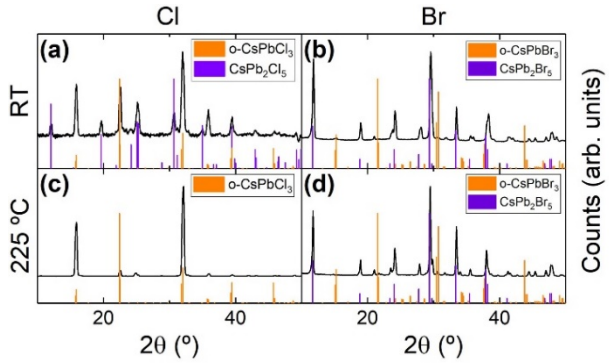

Figure 1. XRD characterization of films prepared by SSVD of $CsCl+PbCl_2$ (a, c) and $CsBr+PbBr_2$ (b, d) at room temperature (a, b) as well as after thermal annealing at 225 °C (c, d). Reference patterns for orthorhombic $CsPbCl_3$ (ICSD-243734), orthorhombic $CsPbBr_3$ (ICSD-97851), as well as $CsPb_2Cl_5$ (ICSD-249888) and $CsPb_2Br_5$ (PDF-25-0211) are shown along the experimental data.

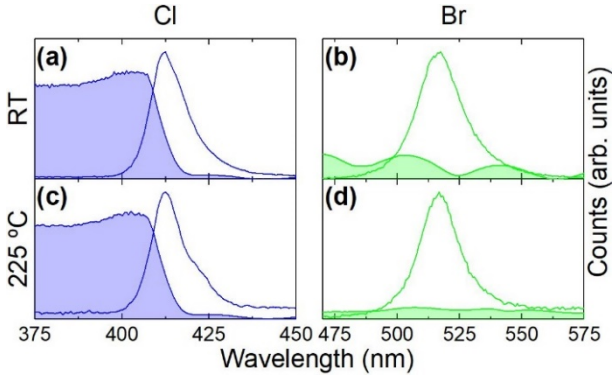

Figure 2. Normalized absorption and photoluminescence spectra of films prepared by SSVD of $CsCl+PbCl_2$ (a, c) and $CsBr+PbBr_2$ (b, d) at room temperature (a, b) as well as after thermal annealing at 225 °C (c, d). The absorption signal present in panel b is linked to optical interferences. Absorption spectra of this film throughout a broader wavelength range can be seen in Figure S1.

As can be seen by X-ray diffraction (XRD, Figure 1) the as-prepared films consist of a mixture of $CsPb_2X_5$ and $CsPbX_3$.[21] However, the

relative amounts of both compounds is different. In the case of the smaller anion (X = Cl), the film is mostly consistent of $CsPbX_3$ (Figure 1a) and exhibits the corresponding absorption onset around 400 nm and Stoke-shifted photoluminescence (PL) centered at 412 nm (Figure 2a).

For the larger anion (X = Br) the $CsPb_2X_5$ compound is dominant (Figure 1b). A close look reveals that reflections characteristics of $CsPbX_3$ are also present although they are broad and not intense. This observation suggests that small domains of $CsPbBr_3$ are embedded in a $CsPb_2Br_5$ matrix. The optical characterization of these films (Figure 2b) shows no marked absorption onset in this range, but only a signal due to optical interferences (see Figure S1 for the full absorption spectrum). However, a rather intense photoluminescence peak centered at 517 nm is visible. This value is slightly blue-shifted from the bulk PL of $CsPbBr_3$.[22] This blue-shift is consistent with the hypothesis of small (tens of nanometers) $CsPbBr_3$ domains in the weak quantum confinement regime,[10] possibly passivated by a $CsPb_2Br_5$ matrix. When the chloride films are annealed at 225 °C, the fraction of $CsPb_2Cl_5$ is substantially reduced so that almost phase-pure $CsPbCl_3$ is obtained (Figure 1c). This is not the case for the bromide films where $CsPb_2Br_5$ remains the dominant crystalline compound (Figure 1d). The optical characteristics of both films remain similar after annealing (Figure 2 c-d). We conclude that SSVD of raw precursors can yield good-quality $CsPbX_3$ perovskites only for the smaller halide (X = Cl), while PbX_2-rich compounds are mainly formed for the larger halide (X = Br). This trend is confirmed by looking at the results of iodide compounds (Figure S2) where no significant $CsPbI_3$ could be formed with this method. In order to obtain higher purity perovskite films by SSVD, we performed dry ball-milling mechanosynthesis of $CsPbX_3$ powders (see supporting information for experimental details). A few recent reports have demonstrated similar mechanosynthesis with highly energetic planetary ball-mills.[17,19] XRD and optical analyses (Figure 3a-c and Figure 4a-c) reveal that ball-milling CsX and PbX_2 compounds at room temperature with a "straight" (non-planetary) setup (see experimental section for more details) results in the formation of high purity $CsPbX_3$ perovskite powders for all halides.

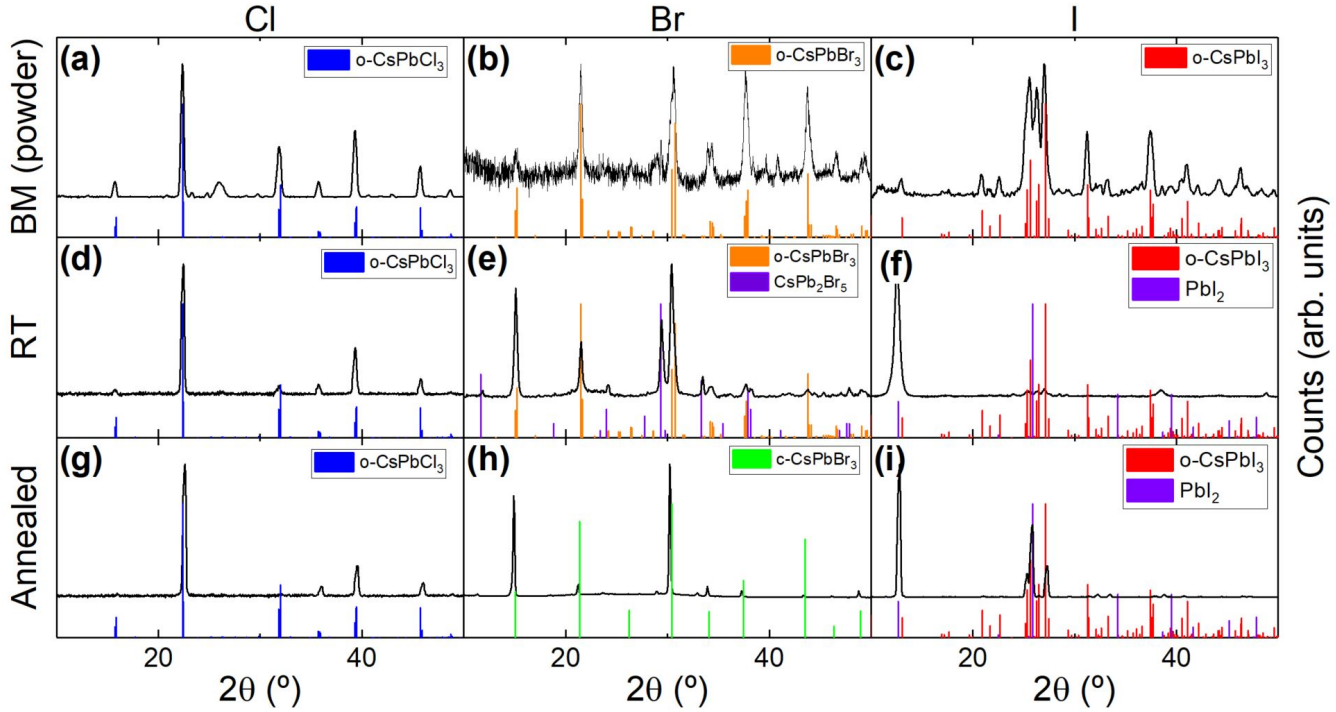

Figure 3. XRD characterization of ball-milled $CsX+PbX_2$ powders (a-c) as well as films prepared by SSVD of the resulting powders at room temperature (d-f) and after thermal annealing (g-i). Note that the annealing temperature is 225 °C for X = Cl and Br (g, h) while it is 325 °C for X = I (i). Reference patterns for orthorhombic $CsPbCl_3$ (ICSD-243734), orthorhombic CsPbBr3 (ICSD-97851), orthorhombic $CsPbI_3$ (ICSD-161480), cubic $CsPbBr_3$ (ICSD-29073), $CsPb_2Br_5$ (PDF-25-0211) and PbI_2 (ICSD-68819) are shown along the experimental data.

When these powders are used for SSVD, the resulting films exhibit a higher purity (*i.e.*, higher relative concentration of $CsPbX_3$) than when non-ball-milled powders are used. This suggests that the pre-formed perovskites sublime at least partially as a single compound ($CsPbX_3$) instead of undergoing a transformation back into CsX + PbX_2 followed by subsequent separate evaporation of both components. Indeed, in the case of the chloride-based compounds, the diffractogram of the film at room temperature (Figure 3d), which is essentially temperature-independent (Figure 3g), shows no signal for $CsPb_2Cl_5$. This means that the purity of the

films deposited at room temperature is already higher than what can be achieved with non-ball-milled precursors even after they were annealed at 225 °C (Figure 1c). The difference is also evident for X = Br. Although $CsPb_2Br_5$ is present in the as-deposited film (Figure 3e), its relative content is much reduced as compared to non-ball-milled samples (Figure 1b). Furthermore, this compound disappears after annealing at 225 °C (Figure 3h; see Figure S3 for XRD characterization at different temperatures) and $CsPbBr_3$ remains the only crystalline compound detectable. This transformation suggests that the original film (before annealing) has an excess of CsBr that can lead to the formation of $CsPbBr_3$ by reacting with $CsPb_2Br_5$.. The other possible hypothesis would be the loss or amorphization of $PbBr_2$, which is unlikely due to its high melting point. The presence of CsBr together with $CsPb_2Br_5$ is hard to detect since its main XRD peak located at $2\Theta = 29{,}38°$ (ICSD: 98–005–3848) overlaps with the signal of $CsPb_2Br_5$, as already noted elsewhere.[21] It must also be noted that no residual powder is left in the crucible after SSVD, which again suggests the presence of excess CsBr in the film before annealing. Previous mechanosynthesis of $CsPbBr_3$ also seems to result in better morphology of the final film (see Figure S4). Indeed, the film prepared from pristine CsBr+$PbBr_2$ mixture presents a patchy morphology at high magnification and cracks are visible at lower magnification. In contrast to this, the film prepared from mechanosynthesized $CsPbBr_3$ shows much higher homogeneity with typical grain sizes of several hundred nanometers. No obvious pinholes can be observed. Iodide perovskites remain the most difficult to form, as previously mentioned. Although mechanosynthesis of the $CsPbI_3$ powder is achieved (see Figure 3c), the resulting films are mainly composed by PbI_2 (Figure 3f). Only after thermal annealing at 325 °C (a higher temperature than used for the chloride and bromide based films), the fraction of $CsPbI_3$ rises significantly, although PbI_2 remains dominant. It must be noted that XRD characterization had to be carried out in air, due to restrictions in our experimental setup, where $CsPbI_3$ is known to degrade.[23,24] This was also observed for the mechanosynthesized $CsPbI_3$ powder. As prepared in nitrogen it is black indicating a cubic crystal structure and when this powder is kept under nitrogen, it remains black (cubic) for over one month (see Figure S5). However, it quickly turns to the "yellow" orthorhombic phase when it is exposed to air before XRD characterization can be completed (Figure 3c). A similar observation is made on the thin film after annealing: the partial conversion to the black phase is clearly visible by eye (Figure S6). It must be noted that the temperature of annealing (325 °C on a hot plate) is close to the phase transition.[25] Hence, it is possible that annealing at higher temperature (which was impossible in our case for technical reasons) might result in a full conversion. When the samples are kept under inert atmosphere (Figure S6) this black phase remains stable for several days.

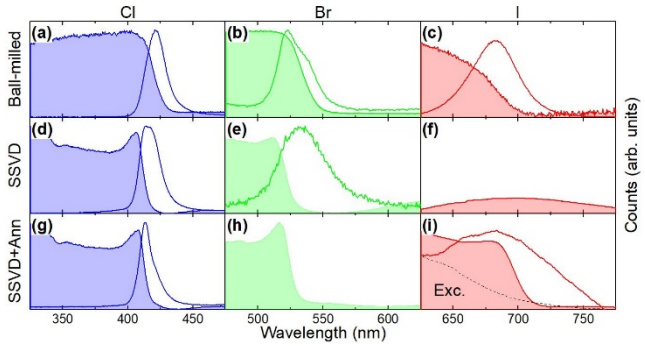

Figure 4. Normalized absorption and photoluminescence spectra of ball-milled $CsX+PbX_2$ powders (a-c) as well as films prepared by SSVD of the resulting powders at room temperature (d-f) and after thermal annealing (g-i). Note that the annealing temperature is 225 °C for X = Cl and Br (g, h) while it is 325 °C for X = I (i). The absorption signal observed in panel f originates from optical interferences. The absorption spectrum of this film throughout a broader wavelength range can be seen in Figure S7.

The optical characterization of the ball-milled powders as well as the resulting films by SSVD is presented in Figure 4. All powders (Figure 4a-c) exhibit the expected absorbance and PL spectra for $CsPbX_3$ compounds, confirming the high quality of mechanosynthesized inorganic halide perovskites. Thin films prepared thereof by SSVD present different characteristics as a function of the halide and temperature. For the smaller chloride anion, the expected absorbance and PL are present both at RT and after annealing at 225 °C, as in the case of non-ball-milled precursors (Figure 2 c,d). For X = Br, a strong absorption onset is visible already at RT (Figure 4e) and gets steeper after annealing (Figure 4h), indicating a higher degree of crystallinity and order in the material. This absorption was not seen in the case of non-ball-milled precursors (Figure 2b-d) and reinforces the conclusion that $CsPbBr_3$ is favored when using previously mechanosynthesized powders while $CsPb_2Br_5$ was mainly formed when using pristine precursors, as previously discussed. We note that the bromide sample shows a weak PL in the as-deposited film (Figure 4e), which is ultimately lost after annealing (Figure 4h). The PL quenching of $CsPbBr_3$ upon thermal annealing is already reported and may be due to the creation of more trap states in the film.[21,26–28] Indeed XRD shows that peaks associated with $CsPbBr_3$ get thinner upon annealing (Figure 3 e,h), which denotes a grain growth. Another possible explanation of the PL loss is linked to higher diffusivity of carriers. As grains become larger upon annealing, it may be expected that diffusion lengths increase and thus electrons and holes can reach surface trap states more easily. Eventually, for the iodide film, no significant absorption or PL is detected at room temperature at the wavelengths of interest (Figure 4f; see Figure S7 for full absorption spectrum). This is consistent with the almost inexistent XRD signal for $CsPbI_3$ in the as-prepared film (Figure 3f). However, after annealing at 325 °C and rapid quenching, a clear absorption onset is visible around 680 nm. PL is also visible though not intense and broad. The broad PL signal is partly attributed to the overlap of the sample's PL with the excitation source which has a weak visible component in addition to the main UV peak at 375 nm, as represented as a reference in Figure 4i).

In summary, we fabricated fully inorganic cesium lead halide thin films by means of fast single-source vacuum deposition (SSVD). We

note that in the case of SSVD of pristine mixed precursors, high-purity perovskite $CsPbX_3$ films could only be obtained for X = Cl after thermal annealing. However, when CsX and PbX_2 are previously ball-milled at room temperature, high purity $CsPbX_3$ powders are formed. SSVD of the so-formed perovskites results in much-improved films both as-prepared as well as after thermal annealing. Perovskite films with optical transitions throughout the visible spectrum from around 400 nm (X = Cl) to around 700 nm (X = I) could be obtained in this way. Thus, we have demonstrated that single-source vacuum deposition of ball-milled perovskites represents an easy, fast and dry process to form high-quality thin films of fully inorganic perovskites. Future work will focus on: (i) implementing these films into different optoelectronic devices such as light-emitting diodes or solar cells, where it will be crucial to avoid chemical impurities and to finely control the film morphology, and (ii) testing the effects of different additives that may work as dopants, passivating agents, or replacement of toxic elements such as lead by other metals such as tin or bismuth.

ASSOCIATED CONTENT

Supporting Information.

The Supporting Information is available free of charge on the ACS Publications website:

Experimental details, XRD and optical characterization of iodide films prepared from pristine precursors, XRD of bromide film under *in-situ* annealing, SEM of bromide films, absorption spectra and photographs of mechanosynthesized $CsPbI_3$ under inert atmosphere and thin films made thereof after annealing and ageing in nitrogen.

AUTHOR INFORMATION

Corresponding Author

*E-mail: Francisco.Palazon@uv.es

Notes

The authors declare no competing financial interest.

ACKNOWLEDGMENT

The research leading to these results has received funding from the European Union Programme for Research and Innovation Horizon 2020 (2014-2020) under the Marie Skłodowska-Curie Grant Agreement PerovSAMs No. 747599, and project INFORM (grant 675867), the Spanish Ministry of Economy and Competitiveness (MINECO) via the Unidad de Excelencia María de Maeztu MDM-2015-0538, MAT2017-88821-R and PCIN-2015-255, and the Generalitat Valenciana (Prometeo/2016/135 and GRISOLIAP/2017/089). H. J. B. acknowledges the support of ERA NET PCIN-2017-014. M. S. thanks the MINECO for his post-doctoral RyC contract.

REFERENCES

(1) Noel, N. K.; Abate, A.; Stranks, S. D.; Parrott, E. S.; Burlakov, V. M.; Goriely, A.; Snaith, H. J. Enhanced Photoluminescence and Solar Cell Performance via Lewis Base Passivation of Organic-Inorganic Lead Halide Perovskites. *ACS Nano* **2014**, *8* (10), 9815–9821.

(2) Stranks, S. D.; Eperon, G. E.; Grancini, G.; Menelaou, C.; Alcocer, M. J. P.; Leijtens, T.; Herz, L. M.; Petrozza, A.; Snaith, H. J. Electron-Hole Diffusion Lengths Exceeding 1 Micrometer in an Organometal Trihalide Perovskite Absorber. *Science (80-.).* **2013**, *342* (6156), 341–344.

(3) Palazon, F.; Pérez-del-Rey, D.; Marras, S.; Prato, M.; Sessolo, M.; Bolink, H. J.; Manna, L. Coating Evaporated MAPI Thin Films with Organic Molecules: Improved Stability at High Temperature and Implementation in High-Efficiency Solar Cells. *ACS Energy Lett.* **2018**, 835–839.

(4) Manser, J. S.; Saidaminov, M. I.; Christians, J. A.; Bakr, O. M.; Kamat, P. V. Making and Breaking of Lead Halide Perovskites. *Acc. Chem. Res.* **2016**, *49* (2), 330–338.

(5) Service, R. F. Cesium Fortifies Next-Generation Solar Cells. *Science (80-.).* **2016**, *351* (6269), 113–114.

(6) Kulbak, M.; Gupta, S.; Kedem, N.; Levine, I.; Bendikov, T.; Hodes, G.; Cahen, D. Cesium Enhances Long-Term Stability of Lead Bromide Perovskite-Based Solar Cells. *J. Phys. Chem. Lett.* **2016**, *7* (1), 167–172.

(7) Sutton, R. J.; Eperon, G. E.; Miranda, L.; Parrott, E. S.; Kamino, B. A.; Patel, J. B.; Hörantner, M. T.; Johnston, M. B.; Haghighirad, A. A.; Moore, D. T.; et al. Bandgap-Tunable Cesium Lead Halide Perovskites with High Thermal Stability for Efficient Solar Cells. *Adv. Energy Mater.* **2016**, *6* (8), 1–6.

(8) Zhang, L.; Yang, X.; Jiang, Q.; Wang, P.; Yin, Z.; Zhang, X.; Tan, H.; Yang, Y. M.; Wei, M.; Sutherland, B. R.; et al. Ultra-Bright and Highly Efficient Inorganic Based Perovskite Light-Emitting Diodes. *Nat. Commun.* **2017**, *8*, 1–8.

(9) Chen, C. Y.; Lin, H. Y.; Chiang, K. M.; Tsai, W. L.; Huang, Y. C.; Tsao, C. S.; Lin, H. W. All-Vacuum-Deposited Stoichiometrically Balanced Inorganic Cesium Lead Halide Perovskite Solar Cells with Stabilized Efficiency Exceeding 11%. *Adv. Mater.* **2017**, *29* (12), 1–7.

(10) Protesescu, L.; Yakunin, S.; Bodnarchuk, M. I.; Krieg, F.; Caputo, R.; Hendon, C. H.; Yang, R. X.; Walsh, A.; Kovalenko, M. V. Nanocrystals of Cesium Lead Halide Perovskites (CsPbX3, X = Cl, Br, and I): Novel Optoelectronic Materials Showing Bright Emission with Wide Color Gamut. *Nano Lett.* **2015**, *15* (6), 3692–3696.

(11) Dirin, D. N.; Cherniukh, I.; Yakunin, S.; Shynkarenko, Y.; Kovalenko, M. V. Solution-Grown $CsPbBr_3$ Perovskite Single Crystals for Photon Detection. *Chem. Mater.* **2016**, *28* (23), 8470–8474.

(12) Ávila, J.; Momblona, C.; Boix, P. P.; Sessolo, M.; Bolink, H. J. Vapor-Deposited Perovskites: The Route to High-Performance Solar Cell Production? *Joule* **2017**, *1* (3), 431–442.

(13) Liu, M.; Johnston, M. B.; Snaith, H. J. Efficient Planar Heterojunction Perovskite Solar Cells by Vapour Deposition. *Nature* **2013**, *501* (7467), 395–398.

(14) Momblona, C.; Gil-Escrig, L.; Bandiello, E.; Hutter, E. M.; Sessolo, M.; Lederer, K.; Blochwitz-Nimoth, J.; Bolink, H. J. Efficient Vacuum Deposited P-i-n and n-i-p Perovskite Solar Cells Employing Doped Charge Transport Layers. *Energy Environ. Sci.* **2016**, *9* (11), 3456–3463.

(15) Longo, G.; Gil-Escrig, L.; Degen, M. J.; Sessolo, M.; Bolink, H. J. Perovskite Solar Cells Prepared by Flash Evaporation. *Chem. Commun.* **2015**, *51* (34), 7376–7378.

(16) Fan, P.; Gu, D.; Liang, G.-X.; Luo, J.-T.; Chen, J.-L.; Zheng, Z.-H.; Zhang, D.-P. High-Performance Perovskite CH3NH3PbI3 Thin Films for Solar Cells Prepared by Single-Source Physical Vapour Deposition. *Sci. Rep.* **2016**, *6* (1), 29910.

(17) Protesescu, L.; Yakunin, S.; Nazarenko, O.; Dirin, D. N.; Kovalenko, M. V. Low-Cost Synthesis of Highly Luminescent Colloidal Lead Halide Perovskite Nanocrystals by Wet Ball Milling. *ACS Appl. Nano Mater.* **2018**, *1* (3), 1300–1308.

(18) Jodlowski, A. D.; Yépez, A.; Luque, R.; Camacho, L.; de Miguel, G. Benign-by-Design Solventless Mechanochemical Synthesis of Three-, Two-, and One-Dimensional Hybrid Perovskites. *Angew. Chemie - Int. Ed.* **2016**, *55* (48), 14972–14977.

(19) Zhu, Z. Y.; Yang, Q. Q.; Gao, L. F.; Zhang, L.; Shi, A. Y.; Sun, C. L.; Wang, Q.; Zhang, H. L. Solvent-Free Mechanosynthesis of Composition-Tunable Cesium Lead Halide Perovskite Quantum Dots. *J. Phys. Chem. Lett.* **2017**, *8* (7), 1610–1614.

(20) Prochowicz, D.; Franckevičius, M.; Cieślak, A. M.; Zakeeruddin, S. M.; Grätzel, M.; Lewiński, J. Mechanosynthesis of the Hybrid

Perovskite CH 3 NH 3 PbI 3 : Characterization and the Corresponding Solar Cell Efficiency. *J. Mater. Chem. A* **2015**, *3* (41), 20772–20777.

(21) Palazon, F.; Dogan, S.; Marras, S.; Locardi, F.; Nelli, I.; Rastogi, P.; Ferretti, M.; Prato, M.; Krahne, R.; Manna, L. From CsPbBr $_3$ Nano-Inks to Sintered CsPbBr $_3$ –CsPb $_2$ Br $_5$ Films via Thermal Annealing: Implications on Optoelectronic Properties. *J. Phys. Chem. C* **2017**, *121* (21), 11956–11961.

(22) Akkerman, Q. A.; Motti, S. G.; Srimath Kandada, A. R.; Mosconi, E.; D'Innocenzo, V.; Bertoni, G.; Marras, S.; Kamino, B. A.; Miranda, L.; De Angelis, F.; et al. Solution Synthesis Approach to Colloidal Cesium Lead Halide Perovskite Nanoplatelets with Monolayer-Level Thickness Control. *J. Am. Chem. Soc.* **2016**, *138* (3), 1010–1016.

(23) Swarnkar, A.; Marshall, A. R.; Sanehira, E. M.; Chernomordik, B. D.; Moore, D. T.; Christians, J. A.; Chakrabarti, T.; Luther, J. M. Quantum Dot–induced Phase Stabilization of A-CsPbI3 Perovskite for High-Efficiency Photovoltaics Abhishek. *Science (80-.).* **2016**, *354* (6308), 92–95.

(24) Liu, F.; Zhang, Y.; Ding, C.; Kobayashi, S.; Izuishi, T.; Nakazawa, N.; Toyoda, T.; Ohta, T.; Hayase, S.; Minemoto, T.; et al. Highly Luminescent Phase-Stable CsPbI3Perovskite Quantum Dots Achieving Near 100% Absolute Photoluminescence Quantum Yield. *ACS Nano* **2017**, *11* (10), 10373–10383.

(25) Moller, C. K. Crystal Structure and Photoconductivity of Caesium Plumbohalides. *Nature* **1958**, *182*, 1436.

(26) Diroll, B. T.; Nedelcu, G.; Kovalenko, M. V.; Schaller, R. D. High-Temperature Photoluminescence of CsPbX $_3$ (X = Cl, Br, I) Nanocrystals. *Adv. Funct. Mater.* **2017**, *27* (21), 1606750.

(27) Palazon, F.; Di Stasio, F.; Lauciello, S.; Krahne, R.; Prato, M.; Manna, L. Evolution of CsPbBr $_3$ Nanocrystals upon Post-Synthesis Annealing under an Inert Atmosphere. *J. Mater. Chem. C* **2016**, *4* (39), 9179–9182.

(28) Yuan, X.; Jing, P.; Li, J.; Wei, M.; Hua, J.; Zhao, J.; Tian, L.; Li, J. Temperature-Dependent Photoluminescence of Inorganic Perovskite Nanocrystal Films. *RSC Adv.* **2016**, *6* (82), 78311–78316.

Insert Table of Contents artwork here